FORMABILITY EFFECTS OF PROCESS PARAMETERS ON FORMING FORCES IN A SINGLE POINT INCREMENTAL FORMING PROCESS (Al-7075)

KISHORE.J[1], MOHANRAJ.A[2], NANDHA KUMAR.R[3], NAVEEN RAJ.A.B[4], MANIKANDAN.K.P[5]

[1,2,3,4-]*UG Student, Department of Mechanical Engineering, SRM VALLIAMMAI ENGINEERING COLLEGE, Tamil nadu, INDIA*

[5-]*Assistant Professor, Department of Mechanical Engineering, SRM VALLIAMMAI ENGINEERING COLLEGE, Tamil nadu, INDIA*

ABSTRACT

Recently, single point incremental forming has caught the attention of automotive and aerospace industry as an alternative to conventional stamping process as an economical process capable of manufacturing sheet metal prototypes devoid of expensive dies. Single point incremental forming (SPIF) is a truly die-less forming process which is quite suitable for the batch type and prototype production due to economical tooling cost, shorter lead time and ability to form non symmetrical geometries without using expensive dies for manufacturing complex components of sheet metal.

1. INTRODUCTION

During the past few years there has been increasing demand for the need of development of manufacturing technologies that are both agile and be able to handle with the market requirements, that is it should be also adaptable for new product development so that introduction of new products in the markets could be easily achieved. Single point incremental forming (SPIF) is a new innovative and feasible solution for the rapid prototyping and the manufacturing of small batch sheet parts. The process is carried out at room temperature and requires a vertical machining center, a square headed tool and a simple support to fix the sheet being formed. The flexibility of the process is mainly related to the fact that SPIF does not require a dedicated die to operate as compared to other forming processes. As a result, the lead-time and cost of tooling along with the die cost can be avoided. This technique allows a relatively fast and cheap production of small series of sheet metal parts. The process starts from a flat sheet metal blank, clamped on a sufficiently stiff rig and mounted on the table of a VMC machine. It can be used for forming of symmetric and non-symmetric parts in a wide range of thicknesses to several mm.

1.1 SINGLE POINT INNCREMENTAL FORMINNG

The emergence of a new sheet metal forming process known as Single Point Incremental Forming (SPIF) has shown great promise in its diversity of use. Relative to other conventional forming processes, SPIF offers more flexibility in forming capabilities and low operating costs. It does not require any dedicated dies and it is ideal for rapid prototyping and low production operations. Forming with this method involves the use of a multi-axis CNC milling machine with a hemispherical tip tool. Unlike its close descendants, shear forming and spinning, SPIF is able to form both axis symmetric and asymmetric shapes because of computer assisted forming. Several advantages are easily realized with this method. Its die less nature and simple forming rig along with the use of generic hemispherical forming tools makes

this process very versatile. Conversely, this is a low volume production method because productivity and cycling time are affected by the size of both the forming tool and the part being formed as well as the type of surface finish that is desired. This rig is mounted to the worktable of the CNC milling machine and it becomes the platform for forming. The clamping and top plates restrict flange material flow into the forming region that is defined by tool path generated from the CAM software.

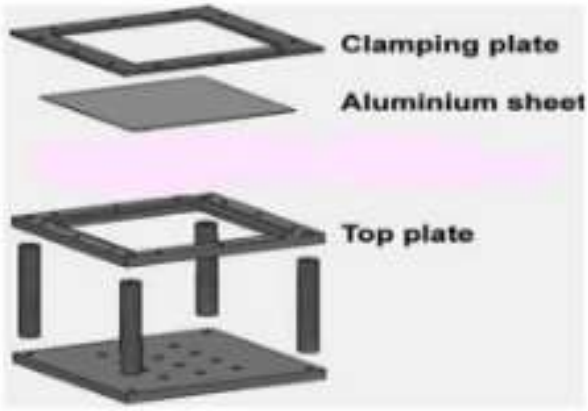

EXPERIMENTAL SETUP

1.2 IMPORTANT FORMING PARAMETERS

In SPIF the following are some of the important process parameters: Tool Path, sheet material, forming angle, tool size, step size, forming speeds (rotation and feed rate), lubrication, and shape. Each parameter is explained below as they pertain to general forming and their respective influences on different observed effects.

1.2.1 FORMING TOOL PATH

In order to form the part with SPIF first we have to generate a cad model and these cad models are utilized for devising the tool paths using commercial CAM software's. The CAD package Solid Edge is used to create solid models of parts that are then imported into the Gibb CAM where the tool path is generated according to the profile of the CAD models. This package is usually used for material removal in milling and is perfect for SPIF because its built-in path generation algorithm can be used to guide the forming tool.Tool contours are created and connected using a step or a spiral transition method.

1.2.2 SHEET MATERIAL

Formability differs between materials and a statistical study by Fratinietal tried to establish the influence of common material properties on formability. From their study, they found that the strain hardening coefficient (n) as well as the interaction between the strength and strain hardening coefficients (K.n), had the highest influence on formability. This study showed that strain hardening coefficient, which differs greatly between materials, had a marked influence on formability. Generally, higher hardening coefficient will have higher formability

1.2.3.TOOL SIZE

Tool size greatly affects both the formability and the surface finish of the manufactured part through this process. Experiments have shown that smaller radius tools have higher formability than larger ones. Larger tools have a bigger contact zone and tend to support the sheet better during forming. Furthermore, in case of larger tool diameters there is an increase in the amount of forming forces due to the increase in contact area between the tool and the metal plate. In case of small diameter tools there is a highly concentrated zone of deformation which results in high strains resulting in better formability. The decreased forces observed with small tools means that lower stresses could be attained and as a result there is smaller probability of the sheet to fail in low stress conditions. Higher formability seen with small radius tools is thought be a consequence of the concentration of force and strain as the surface area of contact is decreased at the tool tip. At this point, frictional heating is very localized and high in magnitude. Both the high heating and strains are thought to allow material to flow easily thus increasing formability.

1.2.4. LUBRICATION AND SHAPE

Lubrication in SPIF research has been limited. Discussions reach only as far as their friction reduction tendencies and as a means to reduce tool wear and improve surface quality as it is a relatively slow process related to machining or milling so tool wear is not one of the major concerns but in case of warm forming lubrication plays a key role in terms of surface roughness's. The geometric shapes that can be formed have a large effect on the forming forces and time depending on complexity. According to the sine law, vertical walls are not possible with this process because it would result in a zero final sheet thickness. Several techniques have been used to improve this limitation including localized heating using laser and multi pass forming. The multi pass method involves forming a part with more than one forming pass. Parts are formed from shallow to increasing angles at each pass until the desired shape is achieved. Forming in multiple steps allows strains within the part to be applied gradually rather than in a single increment.

2.EXPERIMENTAL SETUP

VMC MACHINE

ALIGN KEY

BLANK HOLDER

SCREWS

THE COMPLLETE CLAMPING

TOOL

3.MATERIAL CHARACTERIZATION TABLES

MECHANICAL PROPERTIES OF Al-7075

Property	**Ultimate Tensile Stress ,MPa**	**Yield Strength,MPa**	**Elongation, %**
Nominal	115	106	28
Standard Deviation,σ	0	4	2.5

SELECTED PROPERTIES OF GREASES USED

Grease Type	**ISO Viscosity Grade**	**Average Droping Point,°C(at25°C)**	**Flash point,°C**	**Viscosity at 40°C, ㎡/s**
EP2	ISO VG 15	95	185	15
Kaucuklu	ISO VG 22	89	177	22
Zinol	ISO VG 32	89	174	32
Gp Grease Calcium	ISO VG 46	61	64	46

SELECTED PROPERTIES OF COOLANT OIL USED

Acidity,pH	**Kinematic viscocity at 29°C,㎡/s**	**Boiling Point,°C**
1.086	1.086	95

4. PROGRAM

The idea of the program is simple. Instead of going directly from a CAD model to a helical tool path, a profile tool path is used as an intermediate step. The coordinates of a profile tool path contain information about the geometry and also divides the geometry into layers. The thickness of the layers is the same as the chosen step size. A simple example is used to illustrate how the program calculates the coordinates. Fig. 4 shows the points of two profiles belonging to two subsequent planes or layers of a geometry. For simplicity the number of points in each profile is limited to five and the profiles have been folded out. Points number 1 and 5 are the first

and the last point on the periphery, which are coinciding. To begin with the program calculates the distance between the points in plane 1. They are summed up to Li total see Eq. 1. The program also calculates the distances between each point in plane 1 and all the points in plane 2. As an example, the distance between $P_1$1 and P2,1 is calculated in Eq. 2. This is use by the program to identify which point in plane 2 which is closest to each of the points in plane 1. P21 is identified as the closest point to P_1, in plane 2. The three coordinates for the first helical point are calculated in Eq. 3 to 5. The first helical point becomes the same point as P_1.1. The X coordinates for the second and third helical points are calculated in Eq. 6 and 7. Y and Z coordinates can be calculated in the same way. The X coordinate for the final helical point is calculated in Eq. 8 and this point is the same as P2,5. The helical points and helical tool path are indicated in Fig. 4. The helical points are located where the helical tool path crosses the dashed lines.

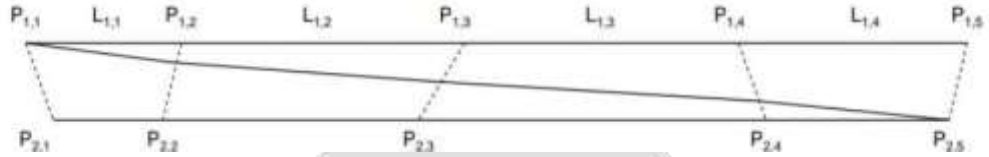

In Fig. 4 the helical tool path is not a straight line between P_1.1 and P2s. For a real profile tool path Litotal will be much larger than the step size which will result in a much more continuous helical tool path.

$$L_{1,Total} = L_{1,1} + L_{1,2} + L_{1,3} + L_{1,4} \quad (1)$$

$$D_{P1,1\ -\ P2,1} = \sqrt{(x_{2,1} - x_{1,1})^2 + (y_{2,1} - y_{1,1})^2 + (z_2 - z_1)^2} \quad (2)$$

$$X_{hel,1} = 0/L_{1,total} * (x_{2,1} - x_{1,1}) + x_{1,1} = x_{1,1} \quad (3)$$

$$Y_{hel,1} = 0/L_{1,total} * (y_{2,1} - y_{1,1}) + y_{1,1} = y_{1,1} \quad (4)$$

$$Z_{hel,1} = 0/L_{1,total} * (z_2 - z_1) + z_1 = z_1 \quad (5)$$

$$X_{hel,2} = L_{1,1}/L_{1,total} * (x_{2,2} - x_{1,2}) + x_{1,2} \quad (6)$$

$$X_{hel,3} = L_{1,1} + L_{1,2}/L_{1,total} * (x_{2,3} - x_{1,3}) + x_{1,3} \quad (7)$$

.

.

.

$$X_{hel,5} = L_{1,1} + L_{1,2} + L_{1,3} + L_{1,4}/L_{1,total} * (x_{2,5} - x_{1,5}) + x_{1,5} = x_{2,5} \quad (8)$$

Generalized expressions for helical coordinates Xheln. YhelnZheln, for a given point n in a given plane p can be seen in Eq. 9 to Eq. 11.

$$Z_{hel,n} = \sum_{i=1}^{n-1} L_{p,i}/L_{p,total} * (Z_{p+1} - Z_p) + Z_p \quad (11)$$

Where Xpe.cl and Ype.cl are the coordinates in the plane p+1 which are closest to the coordinates X and y. in the plane p as seen in Eq. 12. The last term in Eq. 12 could be removed, but is kept so as to use the actual distance. The distance between a given point n in the plane p and the following point n+1 is given in Eq. 13. The total curve length from the first to the last point in the plane p is given in Eq. 14 where t is the total number of points in the plane p.

$$D_{min}=\sqrt{(x_{p+1,cl}-x_{p,n})^2+(y_{p+1,cl}-y_{p,n})^2+(z_{p+1}-z_p)^2} \quad (12)$$

$$L_{p,n}=\sqrt{(x_{p,n+1}-x_{p,n})^2+(y_{p,n+1}-y_{p,n})^2} \quad (13)$$

$$L_{p,total}=\sum_{i}^{i-1} L_{p,I} \quad (14)$$

To get a clear definition of the part, the program preserves the first and the last layer of the profile tool path. This means that the program starts out with a constant Z value for the first layer. As it passes the starting point it starts the helical tool path. When it reaches the lowest Z value it finishes this layer with a constant Z value. In Fig. 5 for illustrative purposes the step size is set to 10 mm for the pyramid and the helical tool path is shown in Fig. 6. Fig. 7 and Fig. 8 compare a section of the tool path for the cone before and after the helical program is used.

5.RESULTS AND DISCUSSION

FORMING FORCES

The influence of four process parameters (sheet thickness, vertical step down size, tool diameter and wall angle) on the tool force was firstly studied by Filice et al. [42] for the cone. They show, through experimental tests, that the tool force increases with increase of all these parameters, as expected. The comparison between experimental and numerical forming tool force evolution is presented, for the cone with wall inclination angle of 45°. Only the vertical component of the forming force is measured experimentally since it presents the higher amplitude. In the current geometry, the sequence of circular tool paths leads to sinusoidal evolutions for both horizontal force components (Fx andFy) measured in the global Cartesian coordinate system. Thus, the horizontal component of the tool force Fx,yis decomposed into tangential and radial directions, as schematically illustrated. This allows evaluation of both the tangential and the radial force amplitude in function of the process time (about 22 min),for the numerical prediction. Tensile yield stress and r value in the sheets plane

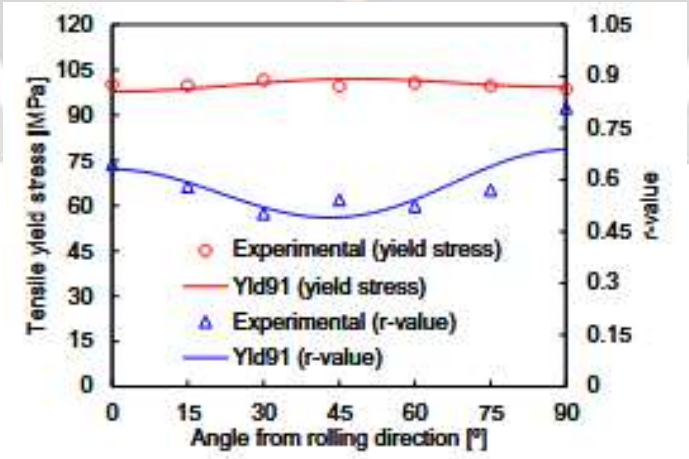

The amplitude of the tangential force (Ft) predicted by the numerical model increases gradually from the beginning of the forming process to attaining the steady state. During this period, bending is the most relevant deformation mechanism. The radial component of the force only reaches the steady state when the contact area of the forming tool is fully evolved, i.e. the slope angle is 45°, which occurs for approximately 600 s of process time. An identical trend is obtained for the vertical (axial) force component, which is in agreement with the experimental result. Nevertheless, the experimental force is slightly overestimated by the finite element model

(see, mainly at the beginning. This difference can result from a small amount of sliding between the metal sheet and the clamping frame, which is not considered in the numerical model. Besides, the force decreases when the kinematic hardening is taken into account, as reported by Flores et al. After reaching the steady state, the forming force remains approximately constant due to the combined effects of strain hardening (force increasing) and thinning (force reduction). Assuming that the tensile strength of this aluminium alloy is198 MPa [44], the axial force value predicted through the empirical equation proposed by Aerens et al. [19] is 1816 N, which is analogous to the steady state value provided by the finite element simulation.

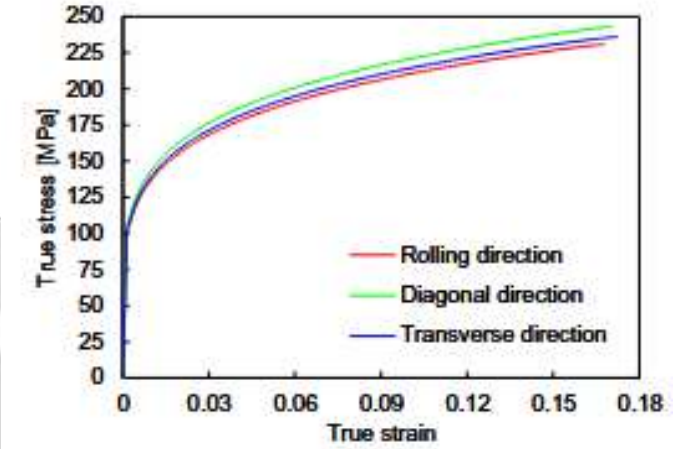

The depth increment between consecutive contours produces a pulse in the experimental force evolution, where the Fz component drops when the tool completes a circular path and then reaches it speak value at the step down increment. The spikes in the numerical tool force evolution were removed for visualization purposes.

6.CONCLUSION

The present study was undertaken with the objective to understand both the deformation mechanism and the stress state imposed on the material during the SPIF process. The truncated cone geometry of AA8006 aluminium alloy, proposed as benchmark in the Numisheet 2014, was selected to validate the proposed finite element model. In order to evaluate accurately the 3D stress distribution under the forming tool, theblank is modelled with solid finite elements in conjunction with an implicit time integration scheme. Additionally, the numerical model takes into account the plastic anisotropy of the aluminium alloy, described by the Yld91 yield criterion.

The experimental forming force is slightly overestimated by the numerical model, which can result from the assumption of isotropic hardening in the mechanical behaviour of the sheet. On the other hand, the final thickness distribution of the truncated cone, predicted by the numerical simulation, is in verygood agreement with the experimental measurements. Indeed, the thickness provided by the finite element simulation is considerably more accurate than the one calculated by the sine law.The comparison between experimental and numerical minor–major strain distribution, evaluated in the exterior surface of the cone, shows that the deformation mode is around plane strain condition. Both the minor and the major plastic strain distributions are accurately predicted by the numerical model ,highlighting the strain path deviation towards biaxial stretchingin the transition zone between the inclined wall and the bottom corner radius of the cone. Due to the action of the forming tool, anegative mean stress is generated in the vicinity of the contact area, postponing the ductile fracture by nucleation and growthof voids. In fact, the strain occurs mainly along the meridional direction

because it is limited in the circumferential direction.Therefore, the residual stresses generated by the cyclic loading arise predominantly in the circumferential direction being positive in the inner skin and negative in the outer skin of the cone.

7.REFERENCES

1. L. Vihtonen1, A. Puzik2, T. Katajarinne3, Comparing Two Robot Assisted Incremental Forming Methods: Incremental Forming by Pressing and Incremental Hammering

2. Ankor Raithatha and Stephen Duncan, An improved finite element model of incremental forming using conic programming, 2008 American Control Conference Westin Seattle Hotel, Seattle, Washington, USA June 11-13, 2008.

3. J.I.V. Sena, R.A.F. Valente and J.J Gracio, Finite element analysis of incrementally formed parts, Int. J. Mechatronics and Manufacturing systems, Vol. 4, No. 5, 2011.

4. S. B. M. Echrif, and M. Hrairi, Research and progress in Incremental sheet forming process, (2010).